

# A theory for the creep of steel fibre reinforced cement matrices under compression

P. S. MANGAT, M. MOTAMED AZARI

*Department of Engineering, University of Aberdeen, Marischal College, Aberdeen, UK*

The paper presents a theoretical model to predict the creep of cement matrices reinforced with randomly oriented discrete steel fibres. The theory considers the composite to be represented by an aligned steel fibre which is surrounded by a thick cylinder of the cement matrix. The fibre provides restraint to the flow component of creep of the matrix through the fibre–matrix interfacial bond strength. The delayed elastic strain component of creep is unaffected by the fibre. The fibre–matrix interfacial bond strength,  $\tau$ , is shown to be primarily a function of the shrinkage of the cement matrix and the radial deformation caused by the sustained axial stress. In addition, the state of stress in the matrix at the interface is suggested to influence greatly the bond strength,  $\tau$ . The validity of the theory is established by means of experimental data on concrete and mortar matrices reinforced with melt extract and hooked steel fibres, at sustained stress–strength ratios of 0.3 and 0.55. Finally an empirical expression is derived to determine the creep of steel fibre reinforced concrete, based on a knowledge of the creep in unreinforced matrices and fibre size and volume fraction.

## 1. Introduction

The creep of cement matrices consists primarily of two components: delayed elastic strain and flowing creep [1]. The delayed elastic component of creep forms a high proportion of creep in the period immediately after the application of the load and it rapidly reaches a limiting value [2]. The flowing creep, however, is very small immediately after the application of the load and continues to increase with time. The introduction of steel fibres does not significantly affect the delayed elastic component of creep, since this deformation is of the same nature as the elastic deformation of concrete which is largely unaffected by steel fibre reinforcement [3]. Steel fibres, however, do provide restraint to the sliding action of the matrix relative to the fibre due to the flow component of creep. This restraint occurs through the fibre–matrix interfacial bond strength.

A creep model for cement matrices reinforced with randomly oriented short steel fibres based on

the concept introduced above is proposed in this paper. Experimental data using hooked and melt extract steel fibres in mortar and concrete matrices, at 0.30 and 0.55 sustained stress–strength ratios, is used to verify the validity of the proposed theory.

A simple empirical expression to predict the creep of steel fibre reinforced at a stress–strength ratio of 0.3 is also derived, based on the creep data presented in this paper.

## 2. Compressive creep theory

### 2.1. Creep model

Creep of concrete under uniaxial compression is comprised primarily of delayed elastic deformation and flow [2]. The introduction of steel fibres in cement matrices is considered to effect significantly the flow component of creep, since the matrix is considered to have a tendency to slide past the fibre and restraint to this sliding action is provided through the interfacial bond. The delayed elastic deformation component of creep

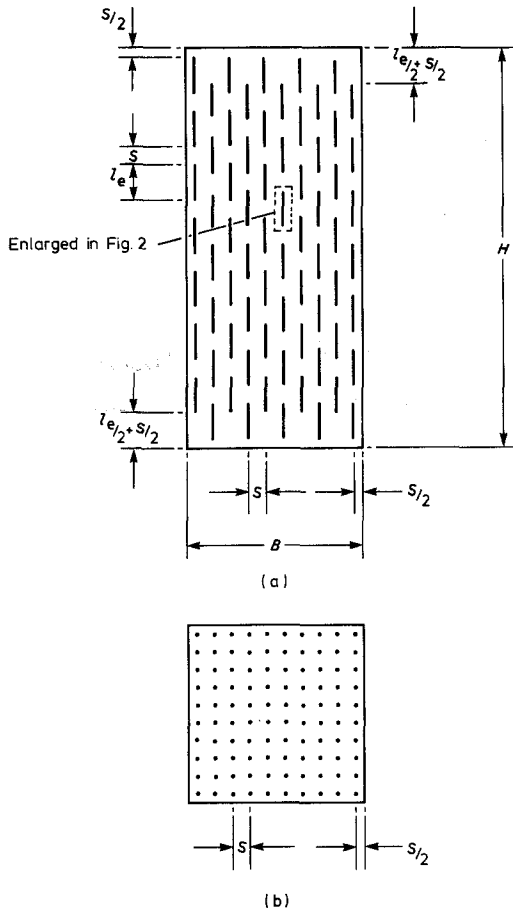


Figure 1 Idealized fibre distribution.

is considered to be unaffected by the fibres. This deformation mode is similar to the elastic case for composite materials, when strain compatibility between the phases is maintained and no relative movement (sliding) occurs between the matrix and fibres.

The idealized distribution of randomly oriented discrete steel fibres in the direction of applied stress is shown in Fig. 1. The spacing between fibres,  $s$ , can be calculated from the following equation which has been derived elsewhere [4]:

$$s^3 + l_e s^2 - B^2(H - l_e/2) \frac{l}{L} = 0 \quad (1)$$

where:  $l$  is the total length of a randomly oriented fibre which yields an effective length  $l_e$  in the direction of stress. The value of  $l_e$  equals  $0.41l$  [5];  $L$  is the equivalent length of a continuous fibre which equals  $4v_f/\pi d^2$  [4];  $v_f$  is the fibre content of the matrix;  $B$  is the specimen breadth; and  $H$  is the specimen height.

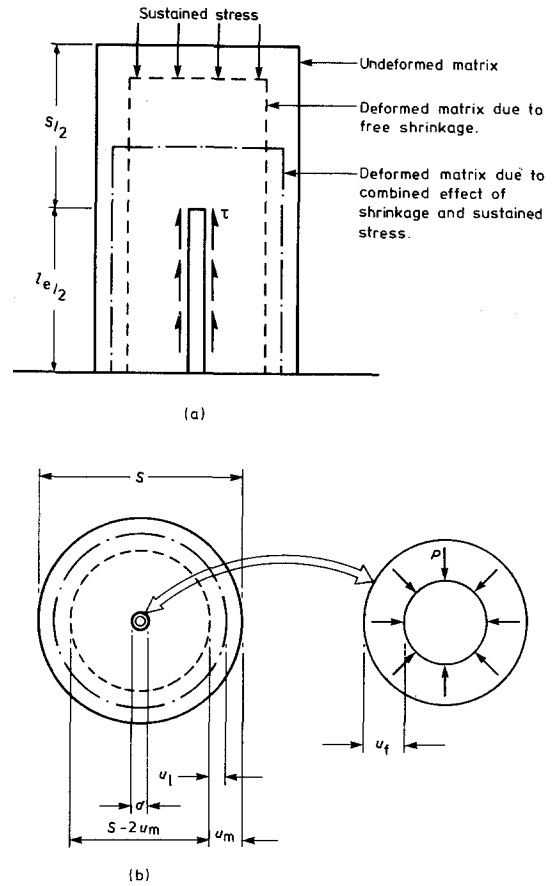


Figure 2 Creep model for fibre reinforced matrices.

The creep model for cement matrices reinforced with randomly oriented short steel fibres of length  $l$  is based on the assumption that aligned fibres of equivalent length  $l_e$  and spacing  $s$ , as shown in Fig. 1, resist creep strains induced in the direction of the applied sustained stress. The element within the dotted area in Fig. 1a is enlarged in Fig. 2 to present a creep model for cement matrices reinforced with randomly oriented steel fibres. As shown in Fig. 2, each fibre is considered to be surrounded by a thick cylinder of cement matrix, of diameter  $s$  and length  $l_e/2 + s/2$ . The deformation of the matrix under sustained stress is represented by the dotted lines in Fig. 2. The interfacial bond stress,  $\tau$ , is mobilized to resist the flow component of creep of the cement matrix.

## 2.2. Theoretical expression for creep of steel fibre reinforced cement matrices

An expression for the creep of steel fibre reinforced cement matrices is obtained from the

model shown in Fig. 2, in terms of the creep of the unreinforced control matrix and the restraint provided by the fibre–matrix interfacial bond, against the flow component of creep of the control cement matrix.

Consider a control cement matrix under a sustained compressive stress  $\sigma$  which causes a total creep strain,  $\epsilon_{0c}$ , in the cement matrix after time,  $t$ . The total creep strain,  $\epsilon_{0c}$ , comprised of a delayed elastic strain component,  $\epsilon_{0d}$ , and a flow component,  $\epsilon_{0p}$ , can be expressed as:

$$\epsilon_{0c} = \epsilon_{0d} + \epsilon_{0p} \quad (2)$$

When the above cement matrix is reinforced with randomly oriented short steel fibres, an element of the composite can be represented by the model in Fig. 2, which is comprised of a single fibre aligned in the direction of applied stress and surrounded by its share of the cement matrix. The creep of the cement matrix is restrained by the steel fibre through the interfacial bond stress,  $\tau$ , as shown in Fig. 2a. This restraint is provided to the flow component of creep,  $\epsilon_{0p}$ , only, delayed elastic strain of the matrix,  $\epsilon_{0d}$ , being unaffected by the presence of the fibre. In order to calculate the creep of the steel fibre reinforced cement matrix element in Fig. 2a, the delayed elastic and flow components of creep of the control matrix are considered separately. Further, deformation due to flow creep is calculated separately for the top zone of the cement matrix of length  $s/2$  (Fig. 2a) which is free of fibre restraint and the bottom zone of the matrix of length  $l_e/2$ , which surrounds the steel fibre and consequently is influenced by its restraint. Hence the total creep deformation  $\delta_{fc}$  of the steel fibre reinforced cement matrix element in Fig. 2a, is determined as the sum of the delayed elastic creep deformation  $\delta_{fd}$ , of the matrix and the flow creep deformation  $\delta'_{fp}$  and  $\delta''_{fp}$  of the top and bottom zones respectively of the matrix described above.

Creep deformation due to delayed elasticity,  $\delta_{fd}$ , of the cement matrix of the fibrous element in Fig. 2a after time  $t$  under a sustained stress  $\sigma$  is given by the expression:

$$\delta_{fd} = \epsilon_{0d} \left( \frac{l_e}{2} + \frac{s}{2} \right) \quad (3)$$

Consider the top zone of the matrix of length  $s/2$ , which is free from fibre restraint. The flow creep deformation of this zone,  $\delta'_{fp}$ , due to the flow component of creep,  $\epsilon_{0p}$ , of the matrix after

time  $t$  under a sustained stress  $\sigma$  is given by the expression:

$$\delta'_{fp} = \epsilon_{0p} \left( \frac{s}{2} \right) \quad (4)$$

The procedure adopted to determine the flow creep deformation of the cement matrix surrounding the fibre in the element shown in Fig. 2a is described below.

The flow creep of the matrix surrounding the fibre is restrained by the fibre through the interfacial bond strength,  $\tau$ . The restraining force,  $R$ , mobilized along the fibre surface due to the flowing action of the matrix past the fibre is given by the expression:

$$R = \pi d \frac{l_e}{2} \tau \quad (5)$$

The restraining force,  $R$ , produces a stress  $\sigma'$  in the matrix surrounding the fibre in a direction opposite to the applied sustained stress  $\sigma$ . Assuming  $\sigma'$  to be uniform in the matrix, its value can be determined from Equation 5 to give:

$$\sigma' = \pi d \frac{l_e}{2} \frac{\tau}{A} \quad (6)$$

where:  $A$  is the cross-sectional area of the matrix surrounding the fibre in Fig. 2a, which equals  $\pi s^2/4$ . Hence, when considering flow creep only, the nett sustained compressive stress,  $\sigma_n$ , acting on the zone of fibre restraint in the element of Fig. 2a is given by:

$$\sigma_n = \sigma - \sigma' \quad (7)$$

substituting for  $\sigma'$  from Equation 6 gives:

$$\sigma_n = \left( \sigma - \pi d \frac{l_e}{2} \frac{\tau}{A} \right) \quad (8)$$

The nett sustained compressive stress,  $\sigma_n$ , on the matrix in the zone of fibre restraint causes a flow creep strain,  $\epsilon_{np}$ , after time  $t$ . The value of  $\epsilon_{np}$  can be determined from a knowledge of the flow creep strain,  $\epsilon_{0p}$ , of the control cement matrix after time  $t$  under a sustained stress  $\sigma$ , by simple proportion. This assumption of a linear relationship between applied sustained stress and flow creep strain is justified by the data of other researchers [1], which is plotted in Figs. 3a and b. A linear relationship between stress and flow creep strain is evident in these figures. This is not surprising since it is well established that elastic strain, total creep strain, and instantaneous creep recovery plus delayed elastic recovery of concrete are linearly related to the stress–strength ratio

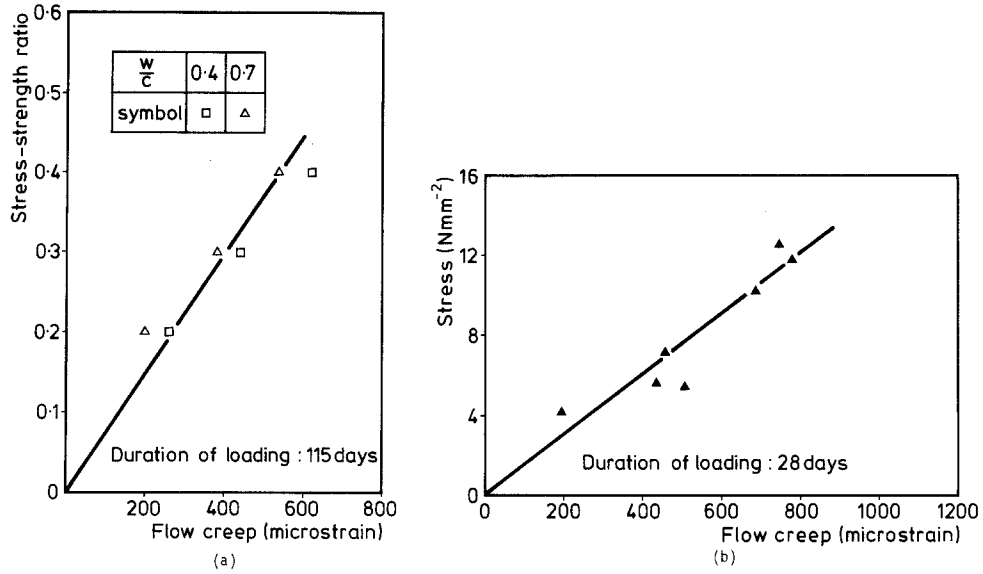


Figure 3 Relationship between sustained stress and flow creep.

[1]. Since flow creep is the algebraic sum of the above strains, its linear relationship with sustained stress is to be expected. In any case the reduction caused in sustained stress in the matrix in the zone of fibre restraint is quite small in practical steel fibre reinforced cement composites. Consequently the difference in the applied stress,  $\sigma$ , and net stress,  $\sigma_n$ , is quite small and, therefore, linear interpolation of their flow creep strains is acceptable regardless of a linear relationship between sustained stress and flow creep. Hence the nett flow creep strain,  $\epsilon_{np}$ , in the fibre restraint zone after time,  $t$ , under sustained stress,  $\sigma_n$ , is given by the expression:

$$\epsilon_{np} = \frac{\sigma_n}{\sigma} \epsilon_{op} \quad (9)$$

where  $\epsilon_{op}$  is the flow creep of the control cement matrix after time  $t$  under a sustained stress  $\sigma$ .

Substituting for  $\sigma_n$  from Equation 8 gives:

$$\epsilon_{np} = \left( \frac{\sigma - \frac{\pi d l_e \tau}{2 A}}{\sigma} \right) \epsilon_{op} \quad (10)$$

which simplifies to:

$$\epsilon_{np} = \left( \epsilon_{op} - \pi d \frac{l_e \tau}{2 A} \frac{\epsilon_{op}}{\sigma} \right) \quad (11)$$

The term  $\sigma/\epsilon_{op}$  may be defined as the stiffness,  $E_c$ , of the control cement matrix against flow creep at time  $t$  under a sustained stress  $\sigma$ . Making

this substitution in Equation 11 gives:

$$\epsilon_{np} = \left( \epsilon_{op} - \pi d \frac{l_e \tau}{2 A E_c} \right) \quad (12)$$

Hence the flow creep deformation,  $\delta''_{fp}$ , of the zone of fibre restraint in Fig. 2a due to flow creep strain  $\epsilon_{np}$  is given by the expression:

$$\delta''_{fp} = \epsilon_{np} \frac{l_e}{2} \quad (13)$$

Substituting for  $\epsilon_{np}$  from Equation 12 gives:

$$\delta''_{fp} = \epsilon_{op} \frac{l_e}{2} - \pi d \left( \frac{l_e}{2} \right)^2 \frac{\tau}{A E_c} \quad (14)$$

Hence the total creep deformation,  $\delta_{fc}$ , of the element of a steel fibre reinforced cement matrix, shown in Fig. 2a, at time  $t$  under a sustained compressive stress  $\sigma$  is given by the expression:

$$\delta_{fc} = \delta_{fd} + \delta'_{fp} + \delta''_{fp} \quad (15)$$

where:  $\delta_{fd}$  is the delayed elastic creep of the cement matrix in Fig. 2a at time  $t$  under a sustained stress  $\sigma$ ;  $\delta'_{fp}$  is the flow creep at time  $t$  under sustained stress  $\sigma$  in the top zone of length  $s/2$ , in Fig. 2a, which does not experience fibre restraint; and  $\delta''_{fp}$  is the flow creep at time  $t$  under sustained stress  $\sigma$  of the cement matrix surrounding the fibre in Fig. 2a, which experiences fibre restraint. Substituting in Equation 15 for  $\delta_{fd}$ ,  $\delta'_{fp}$  and  $\delta''_{fp}$  from Equations 3, 4 and 14 respectively gives:

$$\delta_{fc} = \epsilon_{od} \left( \frac{l_e}{2} + \frac{s}{2} \right) + \epsilon_{op} \left( \frac{s}{2} \right) + \epsilon_{op} \left( \frac{l_e}{2} \right) - \pi d \left( \frac{l_e}{2} \right)^2 \frac{\tau}{AE_c} \quad (16)$$

which simplifies to:

$$\delta_{fc} = \epsilon_{od} \left( \frac{l_e}{2} + \frac{s}{2} \right) + \epsilon_{op} \left( \frac{l_e}{2} + \frac{s}{2} \right) - \pi d \left( \frac{l_e}{2} \right)^2 \frac{\tau}{AE_c} \quad (17)$$

Substituting for  $(\epsilon_{od} + \epsilon_{op}) = \epsilon_{oc}$  from Equation 2 gives:

$$\delta_{fc} = \epsilon_{oc} \left( \frac{l_e}{2} + \frac{s}{2} \right) - \pi d \left( \frac{l_e}{2} \right)^2 \frac{\tau}{AE_c} \quad (18)$$

If the average creep strain in a specimen of the steel fibre reinforced cement composite after time  $t$ , under a sustained compressive stress  $\sigma$ , is  $\epsilon_{fc}$ , then the total creep deformation,  $\delta_{fc}$ , of an element of the material in Fig. 2a, can be expressed as:

$$\delta_{fc} = \epsilon_{fc} \left( \frac{l_e}{2} + \frac{s}{2} \right) \quad (19)$$

which when substituted in Equation 18 gives:

$$\epsilon_{fc} \left( \frac{l_e}{2} + \frac{s}{2} \right) = \epsilon_{oc} \left( \frac{l_e}{2} + \frac{s}{2} \right) - \pi d \left( \frac{l_e}{2} \right)^2 \frac{\tau}{AE_c} \quad (20)$$

Simplifying the above equation and substituting  $A = \pi s^2/4$  and  $l_e = 0.41l$  (5), leads to the following expression for creep of steel fibre reinforced cement matrices:

$$\epsilon_{fc} = \epsilon_{oc} - \frac{0.3362\tau d l^2}{s^2 E_c (0.41l + s)} \quad (21)$$

The solution for  $\epsilon_{fc}$  in the above equation requires a knowledge of  $\tau/E_c$  which is derived in the next section.

### 2.3. Determination of $\tau/E_c$

The nett lateral deformation of the cement matrix in Fig. 2 is the sum of the free shrinkage of the matrix and the lateral deformation caused by the applied sustained stress. The resulting lateral deformation leads to a radial pressure,  $P$ , being exerted on the fibre surface area. The product of this radial pressure and the coefficient of friction,  $\mu$ , between the fibre and matrix gives the magnitude of the average fibre-matrix interfacial bond strength,  $\tau$ .

The value of pressure  $P$  exerted on the fibre surface area is calculated by considering the fibre to cause a virtual radial deformation of the matrix equal to the unrestrained radial shrinkage of the matrix cylinder,  $u_m$ , minus the lateral deformation of the matrix,  $u_1$ , due to the sustained stress and minus the radial deformation of the fibre itself,  $u_f$ , under pressure  $P$ . Hence the virtual deformation of the matrix,  $u$ , can be expressed as:

$$u = u_m - u_1 - u_f \quad (22)$$

The magnitude of the radial deformation of the cylindrical matrix surrounding a single fibre due to the free shrinkage of the matrix, in the absence of any restraint by the fibre, is given as:

$$u_m = \epsilon_{os} \left( \frac{s}{2} - \frac{d}{2} \right) \quad (23)$$

where:  $\epsilon_{os}$  is the free shrinkage strain of the unrestrained control matrix. Equation 23 is based on the assumption that the free shrinkage of the control matrix,  $\epsilon_{os}$ , is uniform throughout the cylindrical matrix.

The radial deformation of the matrix,  $u_1$ , due to the Poisson's effect, which is perpendicular to the direction of the applied sustained stress, is given by the following expression:

$$u_1 = \epsilon_{ol} \left( \frac{s}{2} - \frac{d}{2} \right) \quad (24)$$

where  $\epsilon_{ol}$  is the lateral strain of the unreinforced control matrix. We can define the term  $\epsilon_{ol}$  as:

$$\epsilon_{ol} = \nu_p (\epsilon_{oE} + \epsilon_{oC}) \quad (25)$$

where:  $\nu_p$  is the Poisson's ratio of the unreinforced matrix, which equals 0.2 for both elastic and creep deformation;  $\epsilon_{oE}$  is the elastic strain of the control matrix; and  $\epsilon_{oC}$  is the creep strain of the unreinforced control matrix.

The radial deformation,  $u_f$ , of a fibre under pressure  $P$  can be obtained from the following equation which is based on Lamé's theory for solid cylinders [6]:

$$u_f = \left[ \frac{P(d/2)}{E_s} \right] (1 - \nu_s) \quad (26)$$

where:  $E_s$  is the Young's modulus of steel; and  $\nu_s$  is the Poisson's ratio of steel which equals 0.3.

Hence, substituting in Equation 22 for  $u_m$ ,  $u_1$  and  $u_f$  from Equations 23, 24 and 26 respectively, gives the following expression for the

virtual radial deformation,  $u$ , of the cylindrical matrix:

$$u = \epsilon_{os} \left( \frac{s}{2} - \frac{d}{2} \right) - \epsilon_{ol} \left( \frac{s}{2} - \frac{d}{2} \right) - \left[ \frac{P(d/2)}{E_s} \right] (1 - \nu_s) \quad (27)$$

Alternatively, an expression for the virtual displacement,  $\eta$ , in terms of the radial pressure,  $P$ , generated on the fibre surface, can be obtained by using Lamé's expression for thick cylinders [6] under internal pressure,  $P$ , as follows:

$$u = \left[ \frac{P(d/2)}{E_E} \right] \left[ \frac{(s/2)^2 + (d/2)^2}{(s/2)^2 - (d/2)^2} + \nu \right] \quad (28)$$

where:  $E_E$  is the Elastic modulus of concrete; and  $\nu$  = Poisson's ratio of concrete which equals 0.2. Equating Equations 27 and 28 gives:

$$\left[ \frac{P(d/2)}{E_E} \right] \left( \frac{(s/2)^2 + (d/2)^2}{(s/2)^2 - (d/2)^2} + \nu \right) - \epsilon_{ol} \left( \frac{s}{2} - \frac{d}{2} \right) - \left[ \frac{P(d/2)}{E_s} \right] (1 - \nu_s) \quad (29)$$

which simplifies to:

$$\frac{P}{E_E} = \frac{(\epsilon_{os} - \epsilon_{ol}) [(s/2) - (d/2)]}{\left( \frac{d}{2} \right) \left( \frac{(s/2)^2 + (d/2)^2}{(s/2)^2 - (d/2)^2} + \nu \right) + \frac{(1 - \nu_s)}{(E_s/E_E)}} \quad (30)$$

Also:

$$\tau = \mu P \quad (31)$$

where:  $\mu$  is the coefficient of friction at the steel fibre and cement matrix interface. Therefore, substituting for  $P$  from Equation 30 into Equation 31, leads to the following expression for  $\tau$ :

$$\tau = \frac{\mu E_E (\epsilon_{os} - \epsilon_{ol}) [(s/2) - (d/2)]}{2 \left( \frac{(s/2)^2 + (d/2)^2}{(s/2)^2 - (d/2)^2} + \nu \right) + \frac{(1 - \nu_s)}{(E_s/E_E)}} \quad (32)$$

Dividing both sides of Equation 32 by the stiffness of the flowing matrix,  $E_C$ , leads to the following expression for  $\tau/E_C$ :

$$\frac{\tau}{E_C} = \frac{\mu (\epsilon_{os} - \epsilon_{ol}) [(s/2) - (d/2)] (E_E/E_C)}{2 \left( \frac{(s/2)^2 + (d/2)^2}{(s/2)^2 - (d/2)^2} + \nu \right) + \frac{(1 - \nu_s)}{(E_s/E_E)}} \quad (33)$$

Assuming  $E_E/E_C = \alpha$ , Equation 33 becomes:

$$\frac{\tau}{E_C} = \frac{\alpha \mu (\epsilon_{os} - \epsilon_{ol}) [(s/2) - (d/2)]}{\frac{d}{2} \left( \frac{(s/2)^2 + (d/2)^2}{(s/2)^2 - (d/2)^2} + \nu \right) + \frac{(1 - \nu_s)}{E_s/E_E}} \quad (34)$$

The  $\tau/E_C$  values from Equation 34 can be substituted into Equation 21 to give the creep strain of fibre reinforced matrices.

### 3. Experimental programme

Details of the experimental programme are given in Table I. The mix proportions, by weight, in this investigation were 1:2.5:1.2:0.58 (concrete) and 1:2.75:0:0.58 (mortar). The materials used were Ordinary Portland cement, washed sand conforming to zone 2 of BS 882 and coarse aggregate of 10mm nominal size in accordance with BS 442. Two types of steel fibres were used: melt extract and hooked, details of which are given in Table I.

Prism specimens of size 100 mm × 100 mm × 500 mm were cast in three layers, each layer being compacted on a vibrating table for a few sec. The prisms were then covered with a polythene sheet for 24 h. Subsequently all the prisms, except for concrete prisms reinforced with 1% hooked steel fibres, were cured in a temperature and humidity controlled room for 28 days before being loaded in standard creep rigs. A temperature of 20°C and relative humidity of 55% was maintained in the curing room throughout the test. The concrete prisms reinforced with 1% hooked steel fibres were stored in the laboratory under uncontrolled temperature and humidity throughout. They were cured for 28 days and then loaded up to a stress–strength ratio of 0.3.

Two prism specimens per mix were loaded in each creep rig. Two corresponding unstressed specimens were stored alongside to monitor free shrinkage strains. The load in the creep rigs was applied by means of a hydraulic jack and it was maintained at a constant level by tightening the nuts on the supporting rods. The nut loss was assumed to be 10% of the applied load. The load was topped up regularly throughout the tests. Creep measurements were made by means of a Demec extensometer over a gauge length of 200 mm on the four faces of each prism. The specimens were kept under load for 90 days at sustained stress levels corresponding to 0.3

TABLE I Experimental programme

Mix	Mix proportions	Fibre details			Stress–strength ratio	
		$l$ (mm)	equivalent $d$ (mm)	$v_f$ (%)		Fibre type
$Am_s$		22.5	0.40	1.5, 3	Melt extract (small)	
$Am_l$	1:2.5:1.2:0.58	31.8	0.52	3	Melt extract (large)	0.3
$A_h$		28.2	0.48	1, 3	Hooked	
$A_o$		–	–	0	–	
$Mm_s$		22.5	0.40	3	Melt extract (small)	
	1:2.750:0.58					0.55
$M_h$		28.2	0.48	3	Hooked	
$M_o$		–	–	0	–	
$Am_s$		22.5	0.40	3	Melt extract (small)	
	1:2.5:1.2:0.58					0.55
$A_o$		–	–	0	–	

and 0.55 of the ultimate strength of the prisms, as indicated in Table I. The specimens were then unloaded and creep recovery measurements taken for a further period of up to 60 days.

#### 4. Results and discussion

In the following sections the creep data at sustained stress levels of 0.3 and 0.55 of the ultimate prism strength, as obtained in this investigation, is presented and the influence of steel fibre reinforcement is discussed. This is followed by the determination of  $\tau$ , using Equation 32, by adopting the coefficient of friction,  $\mu$ , values from a previous study of the free shrinkage property of steel fibre concrete [4]. The effect on  $\tau$  of the applied sustained stress and  $v_f(l/d)$  is discussed. This is followed by the determination and comparison of the predicted and experimental values of  $\alpha$  which is the ratio of the elastic modulus of concrete and the stiffness of the flow component of creep. The creep of steel fibre reinforced matrices is then calculated from the proposed theory and comparison made with the experimental results. Finally, by adopting an empirical approach, a simple design expression for the creep of steel fibre reinforced cement matrices is derived.

#### 4.1. Influence of steel fibre reinforcement on the creep of concrete and mortar matrices

The results in Figs. 4 and 5 show the relationship between time under load and creep of concrete and mortar at 0.3 and 0.55 stress–strength ratios. The data in Fig. 4, at 0.3 stress–strength ratio, is for concrete reinforced with different types and volume fractions of steel fibres. The data in Fig. 5 is for steel fibre reinforced mortar and concrete at a stress–strength ratio of 0.55.

The results in Fig. 4 indicate that the addition of steel fibres restrains the creep of concrete at 0.3 stress–strength ratio. Creep progressively decreases as the volume fraction of fibres increases. For example, at 3 vol% of fibres a reduction of about 25% is achieved after 90 days under load.

The results in Fig. 5 show the influence of 3 vol% of fibre reinforcement on the creep of concrete and mortar at 0.55 sustained stress–strength ratio. When comparison of the data for concrete matrices in Fig. 5 is made with the corresponding concrete mixes in Fig. 4, it becomes apparent that steel fibres are less effective in restraining creep at 0.55 stress–strength ratio as compared to creep at 0.3 stress–strength ratio. This is solely due to the fact that at higher

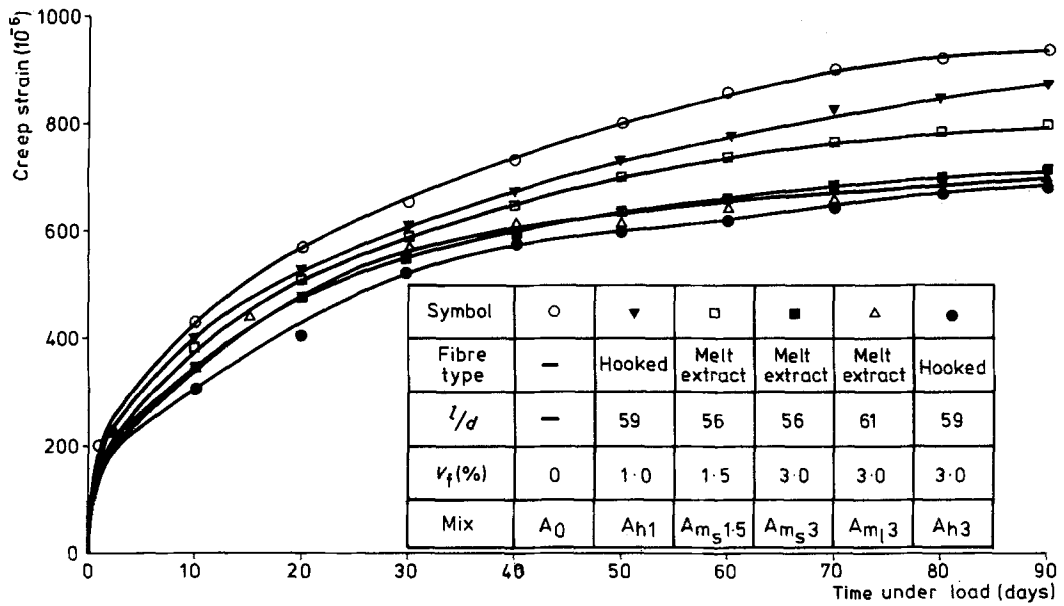


Figure 4 The relationship between creep of fibrous concrete and time under load at 0.3 stress-strength ratio.

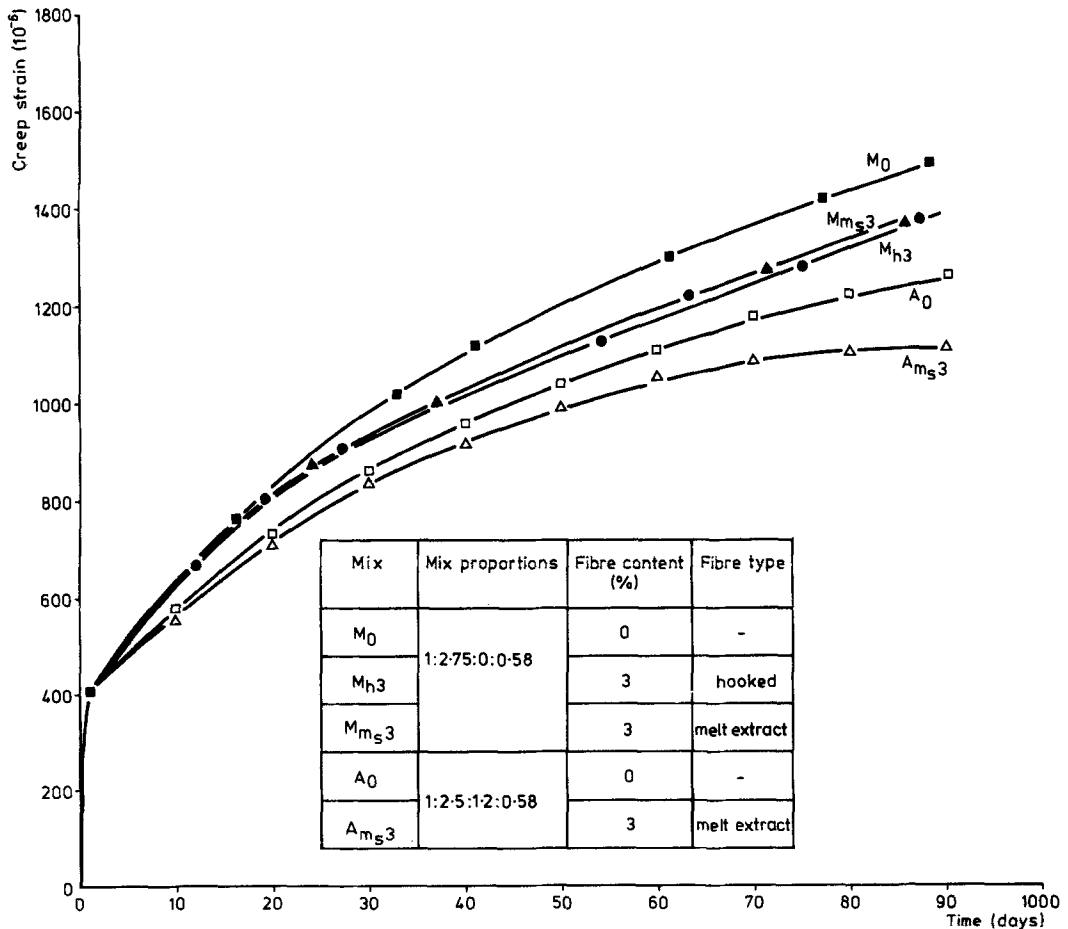


Figure 5 The relationship between creep of fibrous mortar and concrete and time under load at a stress-strength ratio of 0.55.



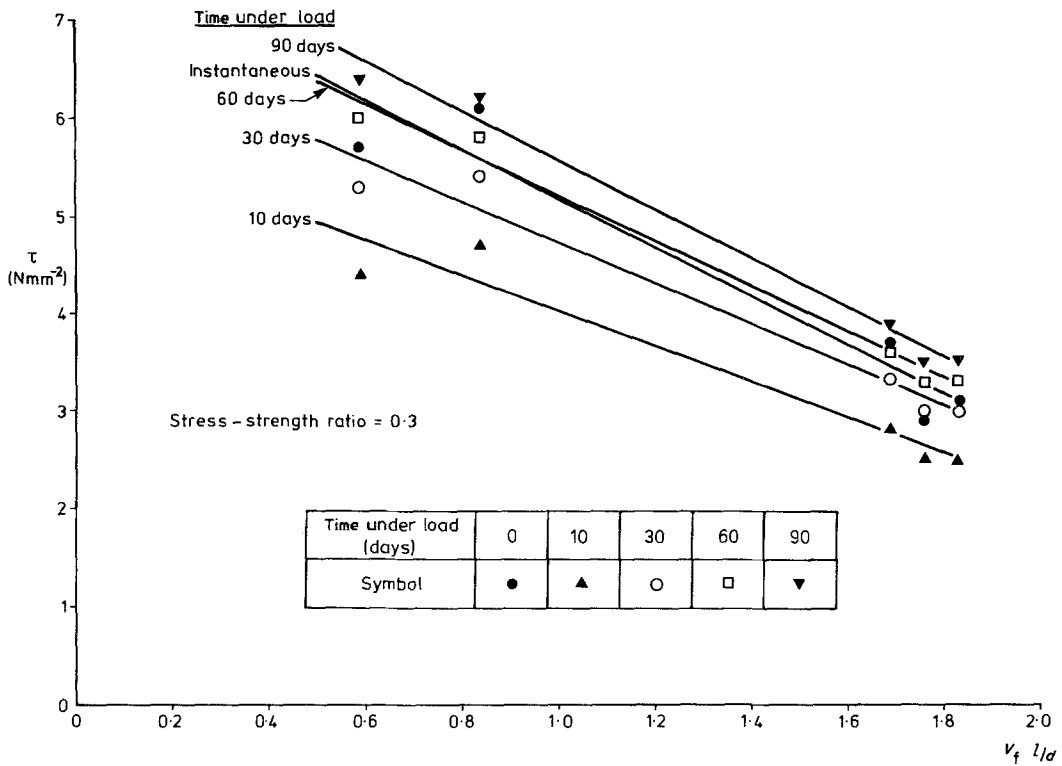


Figure 6 Relationship between  $\tau$  and  $v_f l/d$  for concrete.

sustained stress levels, the magnitude of the lateral strain,  $\epsilon_{ol}$ , is larger which leads to the pressure,  $P$ , in Equation 30 becoming smaller. Since  $\mu$  is constant for a particular type of fibre [4], lower  $P$  values lead to smaller  $\tau$  values in Equation 31, which in turn lead to higher creep strains being predicted from Equation 21.

From the results in Figs. 4 and 5, it can be seen that fibres become more effective in restraining creep of the cement matrices as the time under load increases. This is due to the fact that the flow component of creep becomes more significant later on, with the delayed elastic effect being initially dominant [2]. In addition, the  $\tau$  values increase with time, as is shown in the next section. This leads to more effective restraint by the fibres against the flow component of creep at longer periods under sustained stress.

#### 4.2. Determination of fibre–matrix interfacial bond strength, $\tau$

The fibre–matrix interfacial bond strength values were calculated from Equation 32. The determination of the various parameters in Equation 32 is described below. The values of the coefficient of friction,  $\mu$ , were obtained from a previous

study of the free shrinkage of steel fibre reinforced concrete [4]. The  $\mu$  values for concrete and mortar, reinforced with either hooked or melt extract fibres, are 0.08 and 0.09 respectively. The modulus of elasticity values of concrete and mortar,  $E_E$ , were based on the corresponding cube strength,  $f_{cu}$ , and were determined from the expression [7]:  $E_E = 4.5(f_{cu})^{1/2}$ . The free shrinkage strain of the unreinforced control matrices,  $\epsilon_{os}$ , was obtained from the shrinkage specimens accompanying the creep tests. The total lateral strain values of the control matrices were determined from Equation 24. The remaining parameters in Equation 32 are easily derived.

The results in Figs. 6 and 7 show the influence on  $\tau$  of  $v_f l/d$  and the sustained stress–strength ratio respectively. The data in Fig. 6 indicate that increasing  $v_f l/d$ , leads to significant reduction in  $\tau$  values at the various times under creep loading. This is primarily due to the decrease in fibre spacing caused by increasing  $v_f l/d$ , which leads to thinner cylinders of the cement matrix surrounding each fibre and consequently lower shrinkage deformation [4]. It is also evident, from Fig. 6, that after the instantaneous load there is a reduction in  $\tau$ , as shown by the data

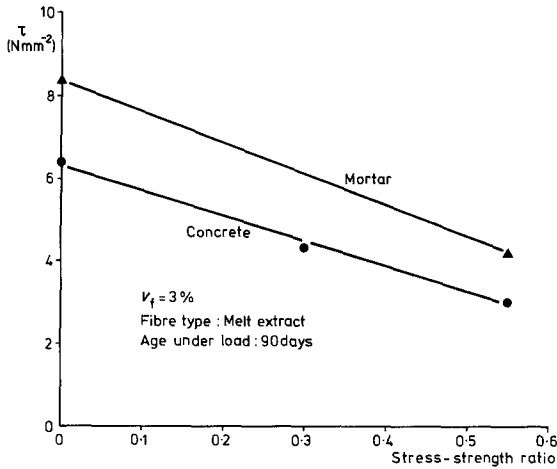


Figure 7 Influence of stress–strength ratio on  $\tau$ .

at 10 and 30 days of creep. This is followed by a gradual increase in  $\tau$ , with time, leading to values greater than the instantaneous value of  $\tau$  as shown by the data at 60 and 90 days under sustained stress. This is due to the fact that within the first few days of loading the free shrinkage strain values in Equation 32 do not increase significantly while the increase in lateral strain,  $\epsilon_{ol}$ , due to the delayed elastic strain component of creep is considerable. This leads to an initial reduction in  $\tau$ . However, with an increase in time under load, the effect of free shrinkage becomes more significant than the lateral strain thus leading to higher  $\tau$  values as seen in Fig. 6.

The results in Fig. 7 show the relationship between the stress–strength ratio and fibre–matrix interfacial bond strength for concrete and mortar reinforced with 3% melt extract fibres after 90 days under load. The stress–strength ratio of zero corresponds to the free shrinkage case [4]. It can be seen that  $\tau$  decreases as the applied sustained stress increases which implies that at higher stress levels steel fibres become less effective in restraining creep of cement matrices. This is due to the fact that as the stress–strength ratio increases the lateral strain,  $\epsilon_{ol}$ , in Equation 25 increases while the free shrinkage strains remain unchanged. This leads to lower fibre–matrix interfacial bond strength values as obtained from Equation 32, and consequently, higher creep of fibre reinforced concrete predicted from Equation 21.

The  $\tau$  values shown in Figs. 6 and 7 are higher than those reported in current literature [8, 9]. This is due to the fact that a compressive state of

stress exists in the matrix at the interface when the composite undergoes compression creep or free shrinkage. Consequently the interfacial bond strength,  $\tau$ , is a function of the compressive stress and strain capacity of the matrix. The  $\tau$  values reported in current literature, however, pertain to the tensile state of stress in the matrix and are, therefore, influenced by the tensile stress and strain capacity which in the case of cement matrices are lower than the corresponding values under a compressive state of stress. For example, the  $\tau$  values reported in current literature range between 0.6 and 13.0 Nmm<sup>-2</sup> as compared with the values obtained under free shrinkage and compression creep which range between 2.3 and 34.5 Nmm<sup>-2</sup> [4].

### 4.3. Determination of $\alpha$

In order to predict the creep of fibre reinforced cement matrices from Equation 21 of the proposed theory, values of the parameter  $\tau/E_C$  are first established from Equation 34. This in turn requires the determination of the factor  $\alpha$ . By definition:

$$\alpha = E_E/E_C \quad (35)$$

where:  $E_E$  is the elastic modulus of concrete; and  $E_C$  is the stiffness of the flowing matrix. Under creep, the applied sustained stress,  $\sigma$ , is constant. Therefore, Equation 35 can be written in the form:

$$\alpha = \frac{(\sigma/\epsilon_E)}{(\sigma/\epsilon_{op})} = \frac{\epsilon_{op}}{\epsilon_E} \quad (36)$$

where:  $\epsilon_E$  is the elastic strain of the control unreinforced cement matrix; and  $\epsilon_{op}$  is the strain corresponding to the flow component of creep of the control matrix.

In Equation 36, the value of  $\epsilon_E$  is provided by the instantaneous strain reading of the creep test on the control mix. In order to determine  $\epsilon_{op}$  the procedure proposed by Illston [2], which considers creep under uniaxial compression to comprise of delayed elastic strain and flow, has been adopted which leads to the equation:

$$\epsilon_{op} = \epsilon_{oc} - \epsilon_{od} \quad (37)$$

where:  $\epsilon_{oc}$  is the total creep strain of concrete; and  $\epsilon_{od}$  is the strain corresponding to the delayed elastic component of creep.

The strain profile of cement matrices under sustained compressive stress, as suggested by

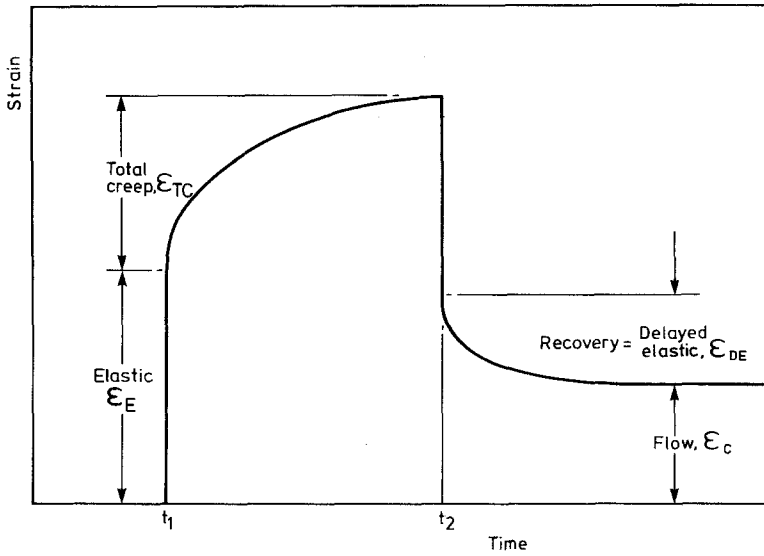


Figure 8 Typical strain profile for concrete under sustained stress.

Illston [2], is shown in Fig. 8. From this it can be seen that the delayed elastic strain component of creep equals the creep recovery strain.

This definition was used to determine the delayed elasticity of the control matrices at unloading after 90 days of creep. The delayed elastic strain component,  $\epsilon_{od}$ , was assumed to remain constant beyond the first ten days of loading [2]. The values of  $\epsilon_{od}$  for mortar and concrete matrices at a stress–strength ratio of 0.55 are 280 and 216 microstrain respectively. The corresponding value at a stress–strength ratio of 0.3, for the concrete control matrix, is 130 microstrain. Hence using the data for  $\epsilon_{oc}$  and  $\epsilon_{od}$  from the standard creep tests on the control matrix, the values of the flow component, of creep,  $\epsilon_{op}$  were determined at various times under load from Equation 37. The experimental values of  $\alpha$  were thus determined by substituting these values of  $\epsilon_{op}$  into Equation 36.

In order to verify the assumptions and reasoning used to derive the creep theory for steel fibre reinforced concrete in this study, another totally independent approach is made to determine the values of  $\alpha$  and comparison made with the experimental  $\alpha$  values as deduced above. This approach uses the theoretical expression for creep given in Equation 21, where the term  $\tau/E_C$  is substituted by its value from Equation 34 to give:

$$\epsilon_{fc} = \epsilon_{oc} - \frac{0.6724l^2 \alpha \mu (\epsilon_{os} - \epsilon_{ol}) [(s/2) - (d/2)]}{s^2 \left( \left( \frac{(s/2)^2 + (d/2)^2}{(s/2)^2 - (d/2)^2} + \nu \right) + \frac{(1 - \nu_s)}{(E_s/E_E)} \right) (0.41l + s)} \quad (38)$$

By substituting the actual creep strains of steel fibre reinforced matrices,  $\epsilon_{fc}$ , and the corresponding strains of control matrices,  $\epsilon_{oc}$ , into Equation 38, the values of  $\alpha$  can be determined since the values of all the remaining parameters in Equation 38 are readily available. Since these values of  $\alpha$  are derived indirectly from the theoretical creep expression, they are termed as the predicted or theoretical values. The experimental and predicted values of  $\alpha$  at a sustained stress–strength ratio of 0.3 are plotted in Fig. 9. The values pertain to concrete matrices reinforced with melt extract and hooked steel fibres at different durations of creep loading of up to 90 days. The results in Fig. 9 show that  $\alpha$  values obtained experimentally and those predicted from the proposed creep expression agree reasonably well. The closest agreement between the experimental and theoretical values of  $\alpha$  is for concrete reinforced with 3 vol% of fibres. Practically all the points which are farthest from the equality line pertain to fibre contents of less than or equal to 1.5 vol%. This close agreement between the experimental and predicted values of  $\alpha$ , for a considerable range of data presented in Fig. 9, confirms the soundness of the proposed creep theory for steel fibre reinforced concrete.

The results in Fig. 10 show the comparison between the experimental and theoretical  $\alpha$  values

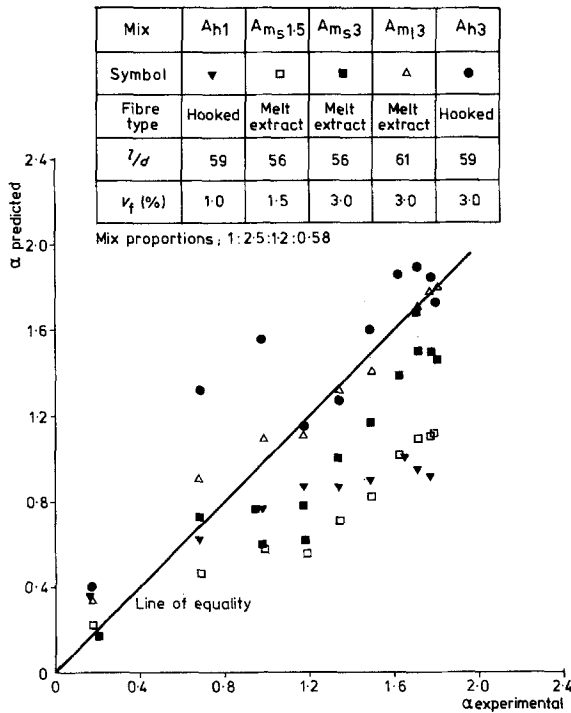


Figure 9 Comparison between the experimental and predicted values of  $\alpha$  for concrete at 0.3 stress-strength ratio.

at 0.55 stress-strength ratio, for concrete and mortar matrices reinforced with 3 vol% melt extract and hooked steel fibres. The correlation between the experimental and theoretical  $\alpha$  values is not nearly as good as the agreement at a stress-strength ratio of 0.3 for the apparent

reason that microcracking plays a very significant role in the creep of concrete at high stress strength ratios [1]. Since the inclusion of fibre reinforcement leads to a greater volume of interfacial cracks [3], microcracking plays a more significant role in the creep of fibre reinforced concrete compared with the control concrete. Hence the theoretical values of  $\alpha$ , obtained from Equation 38, are expected to be less than the experimental values, which is in agreement with the results in Fig. 10.

#### 4.4. Theoretical creep results for steel fibre reinforced cement matrices

Creep strains of steel fibre reinforced cement matrices can be obtained from Equation 21 based on a knowledge of the creep of the unreinforced control matrix,  $\epsilon_{oc}$ , and the term  $\tau/E_C$ . The ratio,  $\tau/E_C$ , is determined from Equation 34 by substituting the experimental values of  $\alpha$  and the  $\mu$  values of 0.08 or 0.09 for concrete and mortar matrices respectively [4]. The remaining factors in Equation 34 are based on standard fibre and matrix properties and on the available information on the free shrinkage of the control matrix and its lateral strains under creep loading. The results in Figs. 11 and 12 show the comparison between the creep strains obtained from the proposed theory and the corresponding experimental results, at 0.3 and 0.55 sustained stress-strength ratios. The data presented are for concrete and mortar matrices reinforced with melt

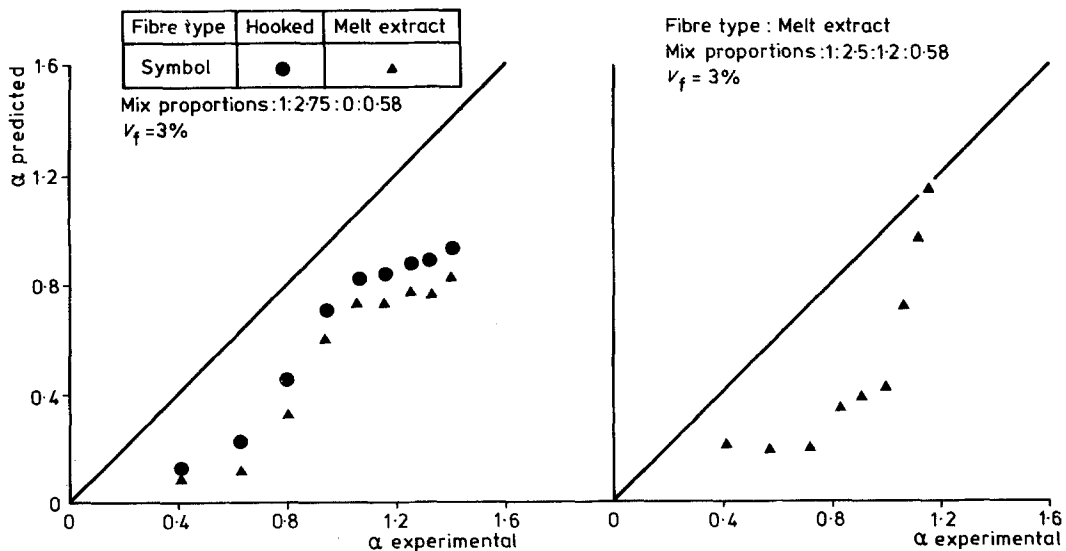


Figure 10 Comparison between the experimental and predicted values of  $\alpha$  for mortar and concrete at 0.55 stress-strength ratio.

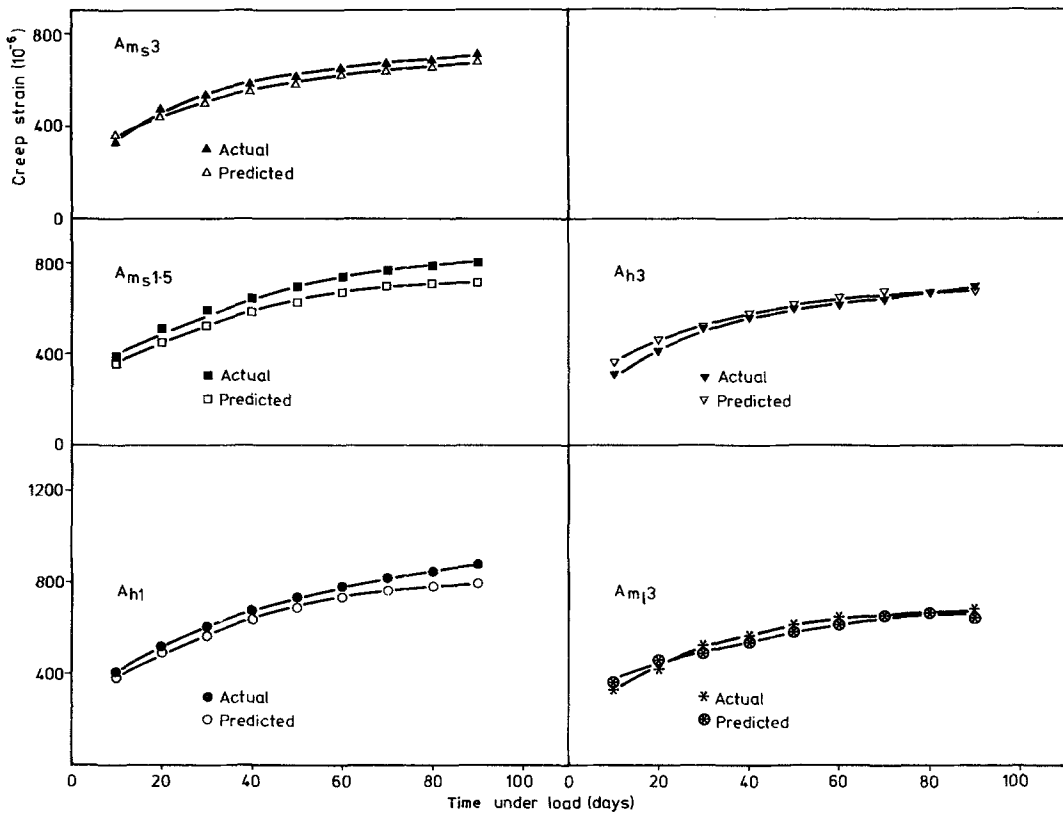


Figure 11 Comparison between the theoretical and experimental creep of fibrous concrete at 0.3 stress-strength ratio.

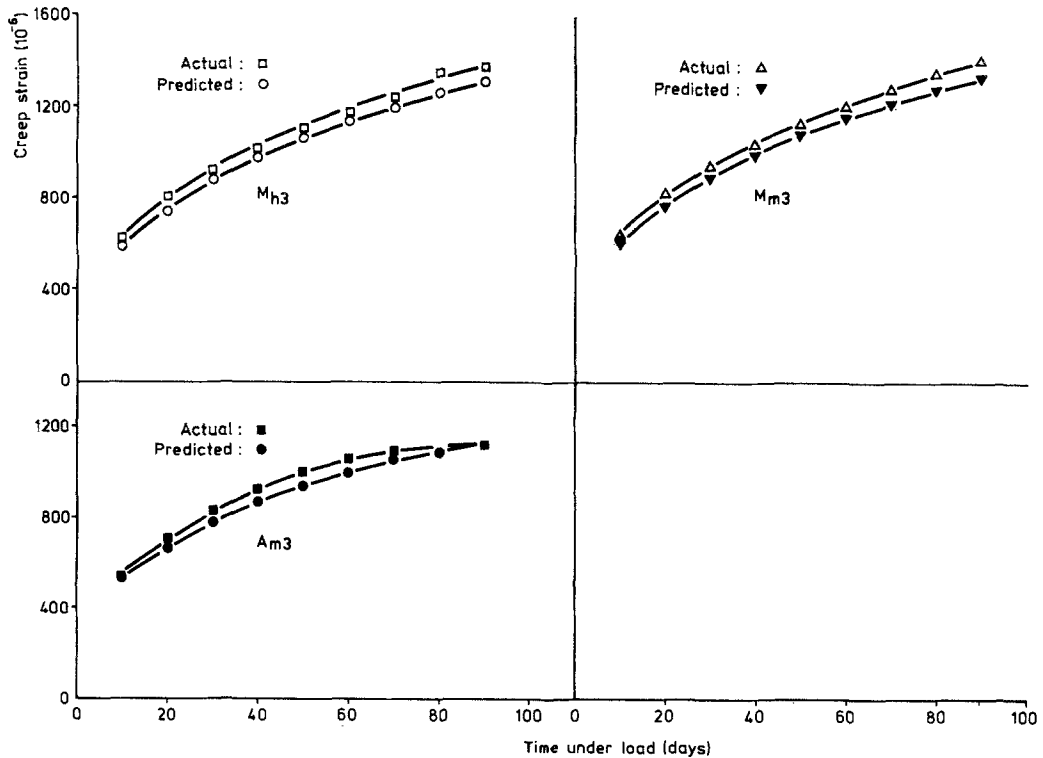


Figure 12 Comparison between the theoretical and experimental creep of fibrous concrete and mortar at 0.55 stress-strength ratio.

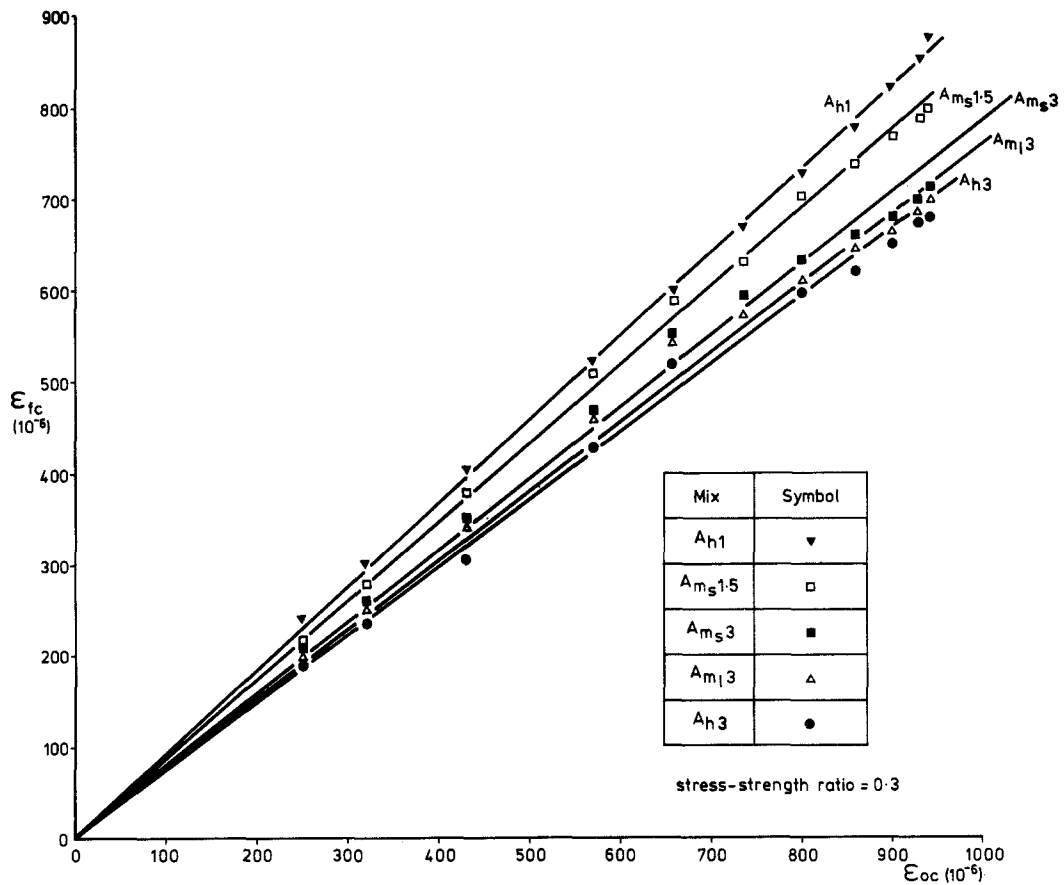


Figure 13 Relationship between the creep of fibre reinforced concrete and unreinforced control concrete.

extract and hooked steel fibres. It is evident in Figs. 11 and 12 that the agreement between the experimental and theoretical results is very satisfactory. The maximum error is about 6% of the mean value.

### 5. Design expression for creep of steel fibre reinforced cement matrices

Although the creep of steel fibre reinforced cement based matrices is predicted satisfactorily by Equation 21 of the proposed theory, it is desirable to obtain a simple design expression for this property. It is found that there exists a linear relationship between the creep of steel fibre reinforced concrete,  $\epsilon_{fc}$ , and the corresponding creep of control matrices,  $\epsilon_{oc}$ , as shown in Fig. 13. The results are for concrete reinforced with different volumes of hooked and melt extract steel fibres, under a sustained stress corresponding to 0.3 of the ultimate prism strength of concrete. From these results it follows that:

$$\epsilon_{fc} = m \epsilon_{oc} \quad (39)$$

where  $m$  is the slope of the graphs between  $\epsilon_{oc}$  and  $\epsilon_{fc}$ .

The slope becomes progressively less as the fibre content increases thus indicating that the reduction in creep due to fibre reinforcement is a function of  $m$ . Further, the values of  $m$ , which are obtained by a linear regression analysis, are related to  $\mu v_f l/d$  as shown in Fig. 14, thus leading to the following relationship:

$$m = 1 - 1.96 \mu v_f \frac{l}{d} \quad (40)$$

A precise expression for the best fit line in Fig. 14 is not possible owing to limited data on the graph. An intercept of unity is assumed in Equation 40 for the obvious reason that at  $\mu v_f l/d = 0$  the composite is, in fact, the control matrix and consequently  $m$  is unity. Substituting for  $m$  from Equation 40 into Equation 39 leads to the following design expression for the creep of steel fibre reinforced concrete at a stress-strength ratio of 0.3.

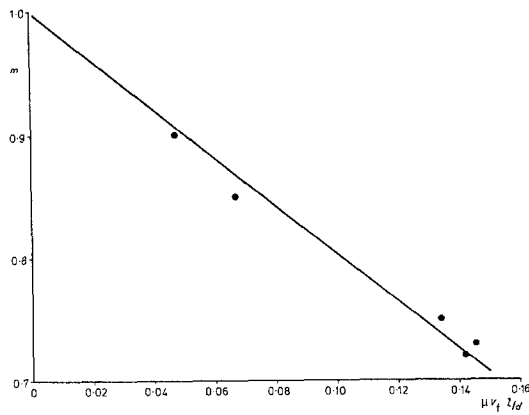


Figure 14 Relationship between  $m$  and  $\mu v_f l/d$  for concrete at 0.3 stress–strength ratio.

$$\epsilon_{fc} = \epsilon_{oc}(1 - 1.96\mu v_f l/d) \quad (41)$$

The creep steel fibre reinforced cement matrices at a stress–strength ratio of 0.3 can hence be obtained simply from Equation 41 based on a knowledge of the creep of the unreinforced matrix and standard parameters of fibre reinforcement. A similar approach can be adopted to derive design expressions at higher sustained stresses. In this investigation, however, data at the higher stress–strength ratio of 0.55 are too limited to enable the derivation of a design expression.

## 6. Conclusions

The proposed theory and model for the compressive creep of cement matrices reinforced with randomly oriented discrete steel fibres is verified by the considerable amount of experimental data presented in this paper. The theory considers that the composite is represented by an aligned steel fibre which is surrounded by a thick cylinder of the cement matrix. The fibre provides restraint only to the flow component of creep of the matrix, through the fibre–matrix interfacial bond strength. The delayed elastic strain component of creep is unaffected by fibre reinforcement.

The fibre–matrix interfacial bond strength,  $\tau$ , is primarily a function of the shrinkage of the cement matrix and the radial deformation caused by the sustained axial stress. In addition, it is influenced by the state of stress in the matrix at this interface. In the case of cementitious matrices,  $\tau$  values under a tensile state of stress at the

interface are smaller than the values under a compressive state of stress. For example, under tension, the  $\tau$  values range between 0.6 and 13.0  $\text{N mm}^{-2}$  whereas under compression, due to creep or shrinkage, the  $\tau$  values range between 2.3 and 34.5  $\text{N mm}^{-2}$ .

Steel fibres are more effective in restraining the creep of cement matrices at low sustained stress–strength ratios owing to smaller lateral deformation caused by the sustained axial stress. This results in greater values of  $\tau$  and hence greater fibre restraint to creep. Also, fibre restraint to creep is more effective later on due to higher shrinkage in the matrix which leads to higher  $\tau$  values and also due to the fact that the flow component of creep becomes more significant with time.

A simple empirical expression,  $\epsilon_{fc} = \epsilon_{oc}(1 - 1.96 \mu v_f l/d)$ , can be used to predict the creep strain,  $\epsilon_{fc}$ , of steel fibre reinforced concrete in terms of the creep of the control concrete,  $\epsilon_{oc}$ . The expression is valid for a sustained stress–strength ratio of 0.3.

## Acknowledgements

The authors gratefully acknowledge the support of the Science and Engineering Research Council, UK, for this work which is part of a larger study on steel fibre reinforced cement matrices.

## References

1. A. M. NEVILLE, "Creep of Concrete—plain, Reinforced and Prestressed" (North Holland Publishing Company, Amsterdam, 1970) pp. 205, 216.
2. J. M. ILLSTON, *Mag. Concr. Res.* 17 (1956) 21.
3. P. S. MANGAT and M. MOTAMED AZARI, *Int. J. Cement Comp. Lightweight Concr.* in press.
4. *Idem*, *J. Mater. Sci.* 19 (1984) 2183.
5. J. P. ROMUALDI and J. A. MANDEL, *ACI* 61 (1964) 657.
6. S. TIMOSHENKO, "Strength of Materials, Part II Advanced Theory and Problems" (C.D. Van Nostrand Co Inc, New York, 1956) p. 205.
7. A. M. NEVILLE, "Properties of Concrete" (Pitman International, London, 1981) p. 312.
8. P. BARTOS, *Int. J. Cement Comp. Lightweight Concr.* 3 (1981) 159.
9. P. S. MANGAT, M. MOTAMED AZARI and B. B. SHAKOR RAMAT, *ibid.* 5 (1983).

Received 29 December 1983  
and accepted 4 June 1984